Simulation of Semiconductor Processes and Devices 2016
Edited by E. Bär, J. Lorenz, and P. Pichler

Modeling Topological-Insulator Field-Effect Transistors using the Boltzmann Equation

William G. Vandenberghe and Massimo V. Fischetti
Materials Science and Engineering
The University of Texas at Dallas, 800 W Campbell Rd, Richardson, TX-75080, USA
E-mail: william.vandenberghe@utdallas.edu

***Abstract*—We model a field-effect transistor making use of the spin-polarized edge states of two-dimensional topological insulators. To account for scattering while respecting Pauli's exclusion principle and the ballistic limit, we employ the Boltzmann equation. We account for phonon-assisted scattering processes and show that the current can be modulated over several orders of magnitude as a function of gate bias.**

INTRODUCTION

To enable downscaling of electronic devices, the requirement of maintaining electrostatic control mandates the introduction of two-dimensional (2D) materials [1]. Many 2D materials are being investigated and presently there is extensive research towards graphene and its analogs such as silicene, germanene [2] and stanene [3], towards transition-metal dichalcogenides in a hexagonal (H), a tetragonal (T) or a distorted tetragonal (T') phase, [4] or towards even more exotic materials such phosphorene [5]. Unfortunately, the purity of these materials is many orders of magnitude removed from the levels of purity we are accustomed to in commercial semiconductor technology and this inevitably limits the performance of these materials in a conventional FET context [6]. Additionally, scattering with out-of-plane (flexural) modes can result in an important reduction in mobilities [7]. Some newly proposed 2D materials however are 2D topological insulators (TIs) [3], [8]–[10], also known as quantum spin Hall insulators, which means they have edge states which are protected against the effects of impurities, defects and edge roughness as well as scattering with phonons.

Recently, we have proposed to use 2D TI edge states to realize field-effect transistors (TIFETs, Fig. 1) by modulating inter-edge scattering [11], [12]. To model these we had relied on a drift-diffusion-like approximation in Ref. [11]. However, the drift-diffusion approach cannot handle the ballistic limit and this poses a challenge when modeling TIFETs. On the other hand, quantum-mechanical ballistic approaches fail because they do not account for scattering. Moreover, quantum-mechanical approaches that do account for scattering often violate Pauli's exclusion principle [13]. We show how the Boltzmann equation can be used to model TIFETs while respecting the ballistic limit, Pauli's exclusion principle, and accounting for scattering.

978-1-5090-0818-6/16/$31.00 ©2016 IEEE

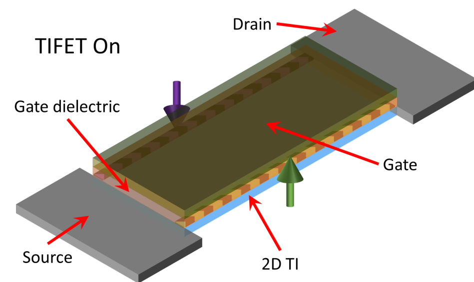

Fig. 1. Schematic of a TIFET in the on-state where current is carried by the edge states and backscattering is prohibited because of spin-momentum locking. In the off-state inter-edge scattering and scattering to "bulk" states is dramatically increased.

TOPOLOGICAL INSULATORS

To obtain the band structure of 2D topological insulators, we rely on the Bernevig-Hughes-Zhang (BHZ) Hamiltonian [8]

$$H = I_2 \otimes \left(\left(\frac{E_g}{2} - \frac{\hbar^2 K^2}{2m} \right) \sigma_3 + \frac{\hbar k_y p}{m_0} \sigma_1 + \frac{\hbar^2 K^2}{2m'} I_2 \right) + \frac{\hbar k_x p}{m_0} \sigma_3 \otimes \sigma_2 \quad (1)$$

where $K = (k_x, k_y)$ is the two-dimensional crystal momentum, E_g is a bandgap, p a momentum matrix element and m and m' are two effective mass parameters. I_2 is the 2×2 identity and $\sigma_{1,2,3}$ are the Pauli matrices. The

Simulation of Semiconductor Processes and Devices 2016
Edited by E. Bär, J. Lorenz, and P. Pichler

values we use are those that yield a band structure similar to that of monolayer tin calculated from first principles [3], [14], [15]: $E_\mathrm{g} = 0.5\,\mathrm{eV}$, $E_p = 2p^2/m_0 = 1.8\,\mathrm{eV}$, $m = 0.08m$ and $m' = 0.12m_0$ where m_0 is the free electron mass. The resulting bulk TI band structure is shown in Fig. 2.

The band structure of a TI ribbon is subsequently determined by discretizing the Hamiltonian ($k_y \rightarrow \mathrm{i}\mathrm{d}/\mathrm{d}y$) and a ribbon with a width (w) of 10 nm is shown in Fig. 3. The states traversing the band-gap are the characteristic – topologically protected – edge states which form the basis of the TIFET operation. The edge states are 2-fold degenerate: one edge state is located on the left edge edge while the other is located on the right edge. The edge states are spin-polarized and time-reversal symmetry ensures that states with opposite momentum ($k_x \rightarrow -k_x$) on the same edge have opposite spin-polarization (↑→↓). As a consequence, scattering processes which conserve spin such as defect/impurity/edge roughness scattering or scattering with phonons can not mediate intra-edge back-scattering. Inter-edge backscattering is allowed but since the wavefunctions associated with the edge states decay exponentially, this process is strongly suppressed for wide ribbons. The decay length depends on the energy and the inter-edge overlap integrals are the smallest for states with an energy near the middle of the bandgap.

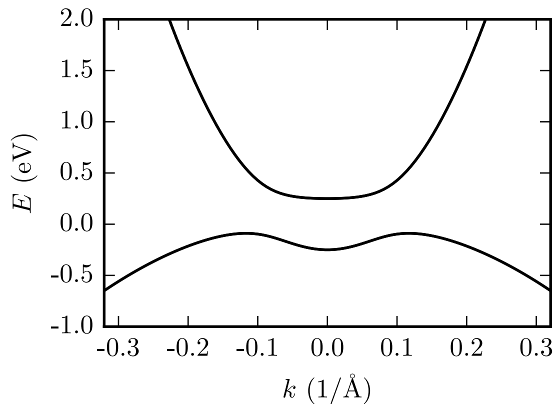

Fig. 2. Bulk topological insulator band structure with a bandgap of 0.33 eV similar to the bandgap of functionalized monolayer tin.

BOTLZMANN EQUATION

To study the electronic transport in a FET structure, accounting for scattering while respecting the ballistic limit and Pauli's exclusion principle, we solve the one-dimensional Boltzmann equation

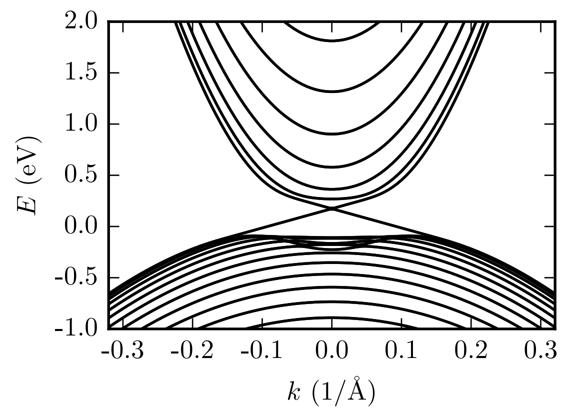

Fig. 3. 10 nm topological insulator ribbon band structure. The states traversing the bulk bandgap in the ribbon band structure are the topologically protected spin-polarized edge states.

$$\frac{\mathrm{d}E_j(k)}{\mathrm{d}\hbar k}\frac{\partial f_j(x,k)}{\partial x} + \frac{\mathrm{d}V(x)}{\hbar\mathrm{d}x}\frac{\partial f_j(x,k)}{\partial k} + \sum_{j'}\int \mathrm{d}k' \Big((1-f_j(x,k))S_{jj'}(k,k')f_{j'}(x,k') - (1-f_{j'}(x,k'))S_{j'j}(k',k)f_j(x,k)\Big) = 0 \quad (2)$$

where $f_j(x,k)$ is the Boltzmann distribution, x denotes the transport direction, and $k = k_x$, $E_j(k)$ is the electron dispersion (in our case for the TI) for subband j and $S_{jj'}(k,k')$ is the scattering rate. We discretize along the reciprocal space with n_k points and use central difference. Along the real-space direction we use n_x points and use a finite element approach, applying boundary conditions at $x = 0$ and at $x = L$ so that $f_j(x,k)$ equals the Fermi-Dirac distribution when electrons are injected in the device.

We include the electron-phonon scattering rate through

$$S_\mathrm{ph}^\mathrm{em,abs}(k,k') = DK^2\frac{1}{2\rho\omega}\left(\frac{1}{2}\mp\frac{1}{2}+N(\hbar\omega)\right) \times |M(k,k')|^2\delta\left(E(k)-E(k')\right) \quad (3)$$

where DK is the deformation potential determined from first principles [16], ρ the mass density per unit length, ω the phonon frequency,

$$M(k,k') = \sum_\alpha \int \mathrm{d}y\, \phi_k^{\alpha *}(y)\phi_{k'}^{\alpha}(y) \quad (4)$$

the matrix element determined from the ribbon wavefunctions $\phi_k^\alpha(y)$, and α the index running over the four discrete degrees of freedom of the bulk Hamiltonian.

For the acoustic phonons, we assume elastic scattering and the electron-phonon scattering rate simplifies to $S_{\mathrm{ph,el}}(k,k') = \Delta^2 kT|M(k,k')|^2/(\hbar 2\rho v_{\mathrm{s}}^2|\mathrm{d}E/\mathrm{d}k|)\delta(k+k')$ where $\Delta = \mathrm{d}DK/\mathrm{d}k$. Here we assume a linear energy dispersion for the phonon energy $\hbar\omega = v_{\mathrm{s}}q$ while in reality, the out-of-plane (ZA) and the transversal (TA) acoustic phonons will have a parabolic dispersion possibly leading to much larger scattering rates. [7]

Since Eq. (2) is a non-linear equation because of the Pauli exclusion (often ignored [17]) in the scattering terms, we solve it by iterations using Newton's method. The Jacobian can be calculated exactly by differentiating the left hand side of Eq. (2). As an initial guess for the distribution function we take either the distribution from the contacts or the distribution function from a previous iteration. Convergence of Newton's method is not always obtained when a coarse x or k mesh is used in addition to large discretization errors. At the same time there is an upper limit on the mesh size because of the size of the Jacobian and the associated memory constraints. In our case, a good compromise was found by using 160 k-points and 80 x-points.

To obtain the potential distribution $V(x)$, we solve Poisson's equation in two dimensions (x,z) with a source and drain bias applied on the left ($x = 0$) and right ($x = L$) and a gate bias in a gate region on the top and bottom ($|z| = t/2$, $|x - L/2| < L_{\mathrm{gate}}/2$). Since the self-consistent solution of Poisson's equation with the Boltzmann equation requires the solution of an additional non-linear problem, for convenience we presently limit ourselves to a non-selfconsistent approach ignoring the charge in the channel in the Poisson equation. The non-selfconsistent approach can be expected to be a better approximation as devices are smaller and have a higher dielectric constant.

In Fig. 4, we show the Boltzmann distribution function $f_j(x,k)$ of the edge states for $L = 3\,\mu\mathrm{m}$, $L_{\mathrm{gate}} = 1\,\mu\mathrm{m}$, $V_{\mathrm{gs}} = 0.36$ V and $V_{\mathrm{ds}} = 0.1$ V as an illustration of a typical solution. Because of the gate bias, the electrons accelerate away from the source towards the gate region. In the gate region, states with higher energy are occupied and the asymmetry of the distribution function between positive and negative momentum results in a non-vanishing current.

To clarify how current is carried in the device, we show the "net velocity" of electrons with opposite momentum $v(k)\,(f(x,k) - f(x,-k))$ in Fig. 5. The limiting factor for the current through the TIFET is determined by the scattering under the gate region. The scattering rate is very small for energies in the bulk TI bandgap (small k) but increase rapidly for energies closer to the bulk TI band edges (increasing k).

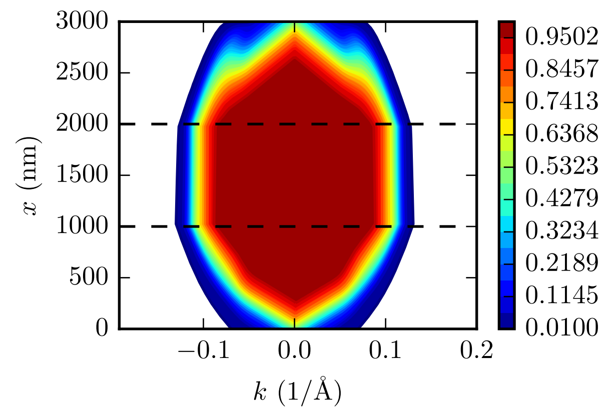

Fig. 4. Boltzmann distribution for the first conduction band in a TIFET with $L = 3\mu m$, $L_{\mathrm{gate}} = 1\mu m$, $V_{\mathrm{gs}} = 0.36$V and $V_{\mathrm{ds}} = 0.1$V . The gate bias makes the charge density larger in the gate region (1000-2000 nm) compared to the source and drain regions.

In Fig. 6, we show the calculated current

$$J = \int \frac{\mathrm{d}k}{2\pi}\, v(k) f(x,k) \tag{5}$$

(which is independent of x) as a function of gate bias confirming the previously predicted switching behavior for the TIFET based on the modulation of scattering in the TI by changing the gate bias. Overall, using the parameters used in this study, the simulated ratio between on and off current is 2 orders of magnitude. In the on-state (gate bias between -0.2 V and 0.1 V), electrons travel ballistically through the edge states since the overlap for intra-egde scattering vanishes (time-reversal symmetry) and the overlap for inter-edge scattering is very small (exponential decay in the bandgap). In the off-state, the intra-edge scattering becomes much stronger since the edge state energies are no longer in the gap and the wavefunctions do not decay exponentially anymore. Stronger scattering with phonons or scattering with impurities will lead to a reduction of the off-current while the impact on the on-current will be minimal.

Conclusion

The Boltzmann equation can be solved exactly for one-dimensional structures yielding an approach capable of dealing with scattering and Pauli's exclusion principle while respecting the ballistic limit. Using this approach, we show that the TIFET maintains its switching behavior after taking the ballistic limit into account. Using the topologically protected edge states to deliver the drive

current ensures that the TIFET will maintain its high quasi-ballistic on-current even in the presence of defects or impurities.

Acknowledgements

We acknowledge the support of Nanoelectronics Research Initiative's (NRI's) Southwest Academy of Nanoelectronics (SWAN).

References

[1] M. V. Fischetti, B. Fu, and W. G. Vandenberghe, "Theoretical study of the gate leakage current in sub-10-nm field-effect transistors," *IEEE Transactions on Electron Devices*, vol. 60, no. 11, pp. 3862–3869, 2013.

[2] M. Houssa, E. Scalise, K. Sankaran, G. Pourtois, V. Afanas'Ev, and A. Stesmans, "Electronic properties of hydrogenated silicene and germanene," *Applied Physics Letters*, vol. 98, no. 22, p. 223107, 2011.

[3] Y. Xu, B. Yan, H.-J. Zhang, J. Wang, G. Xu, P. Tang, W. Duan, and S.-C. Zhang, "Large-gap quantum spin hall insulators in tin films," *Physical review letters*, vol. 111, no. 13, p. 136804, 2013.

[4] Q. H. Wang, K. Kalantar-Zadeh, A. Kis, J. N. Coleman, and M. S. Strano, "Electronics and optoelectronics of two-dimensional transition metal dichalcogenides," *Nature nanotechnology*, vol. 7, no. 11, pp. 699–712, 2012.

[5] H. Liu, A. T. Neal, Z. Zhu, Z. Luo, X. Xu, D. Tománek, and P. D. Ye, "Phosphorene: an unexplored 2d semiconductor with a high hole mobility," *ACS nano*, vol. 8, no. 4, pp. 4033–4041, 2014.

[6] S. McDonnell, R. Addou, C. Buie, R. M. Wallace, and C. L. Hinkle, "Defect-dominated doping and contact resistance in mos2," *ACS nano*, vol. 8, no. 3, pp. 2880–2888, 2014.

[7] M. V. Fischetti and W. G. Vandenberghe, "Mermin-wagner theorem, flexural modes, and degraded carrier mobility in two-dimensional crystals with broken horizontal mirror symmetry," *Physical Review B*, vol. 93, no. 15, p. 155413, 2016.

[8] B. A. Bernevig, T. L. Hughes, and S.-C. Zhang, "Quantum spin hall effect and topological phase transition in hgte quantum wells," *Science*, vol. 314, no. 5806, pp. 1757–1761, 2006.

[9] M. König, S. Wiedmann, C. Brüne, A. Roth, H. Buhmann, L. W. Molenkamp, X.-L. Qi, and S.-C. Zhang, "Quantum spin hall insulator state in hgte quantum wells," *Science*, vol. 318, no. 5851, pp. 766–770, 2007.

[10] X.-B. Li, W.-K. Huang, Y.-Y. Lv, K.-W. Zhang, C.-L. Yang, B.-B. Zhang, Y. Chen, S.-H. Yao, J. Zhou, M.-H. Lu, *et al.*, "Experimental observation of topological edge states at the surface step edge of the topological insulator zrte 5," *Physical review letters*, vol. 116, no. 17, p. 176803, 2016.

[11] W. G. Vandenberghe and M. V. Fischetti, "Realizing a topological-insulator field-effect transistor using iodostannanane," in *2014 IEEE International Electron Devices Meeting*, pp. 33–4, IEEE, 2014.

[12] W. G. Vandenberghe and M. V. Fischetti, "Calculation of room temperature conductivity and mobility in tin-based topological insulator nanoribbons," *Journal of Applied Physics*, vol. 116, no. 17, p. 173707, 2014.

[13] R. Lake, G. Klimeck, R. C. Bowen, and D. Jovanovic, "Single and multiband modeling of quantum electron transport through layered semiconductor devices," *Journal of Applied Physics*, vol. 81, no. 12, pp. 7845–7869, 1997.

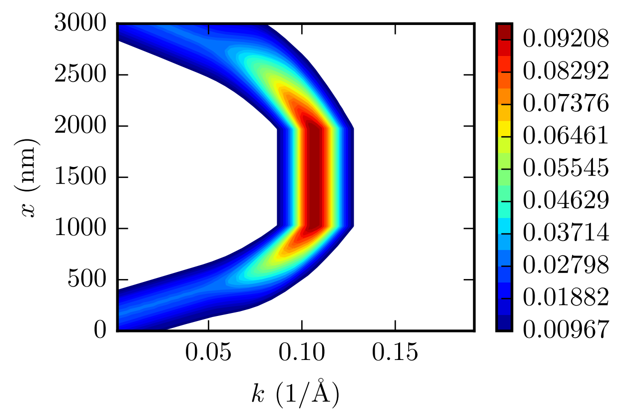

Fig. 5. "Net velocity" of electrons with opposite momentum $v_j(k)\,(f_j(x,k) - f_j(x,-k))$ in the first conduction band. Comparing with Fig. 4, we can see that the current is carried by those states where the distribution makes a transition from 0 to 1.

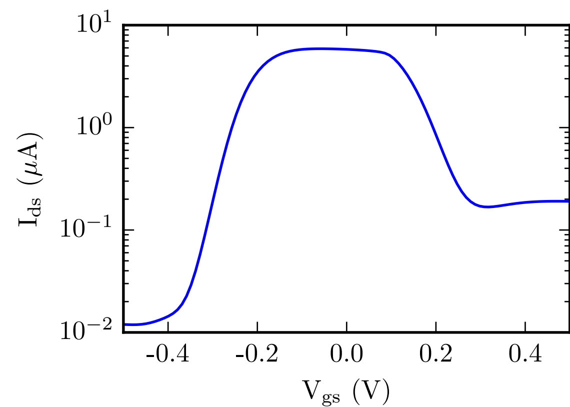

Fig. 6. Input characteristic of a TIFET obtained by solving the Boltzmann equation for 0.1 V drain-source bias. When the gate bias is around 0 V, scattering is minimal and electrons travel through the channel quasi-ballistically. When the gate bias moves the Fermi level into the bulk conduction or valence band, scattering is increased and the current decreases.

[14] A. S. Negreira, W. G. Vandenberghe, and M. V. Fischetti, "Ab initio study of the electronic properties and thermodynamic stability of supported and functionalized two-dimensional sn films," *Physical Review B*, vol. 91, no. 24, p. 245103, 2015.

[15] G. Kresse and J. Hafner, "Ab initio molecular dynamics for liquid metals," *Physical Review B*, vol. 47, no. 1, p. 558, 1993.

[16] W. G. Vandenberghe and M. V. Fischetti, "Deformation potentials for band-to-band tunneling in silicon and germanium from first principles," *Applied Physics Letters*, vol. 106, no. 1, p. 013505, 2015.

[17] S. Jin, M. V. Fischetti, and T.-w. Tang, "Theoretical study of carrier transport in silicon nanowire transistors based on the multisubband boltzmann transport equation," *IEEE Transactions on Electron Devices*, vol. 55, no. 11, pp. 2886–2897, 2008.

[18] X. Qian, J. Liu, L. Fu, and J. Li, "Quantum spin hall effect in two-dimensional transition metal dichalcogenides," *Science*, vol. 346, no. 6215, pp. 1344–1347, 2014.